Available online at www.sciencedirect.com
ScienceDirect
Ceramics International 35 (2009) 2329–2335
CERAMICS INTERNATIONAL
www.elsevier.com/locate/ceramint

Fabrication of 8-YSZ thin-wall tubes by powder extrusion moulding for SOFC electrolytes

T. Jardiel [a], B. Levenfeld [a], R. Jiménez [b], A. Várez [a,*]

[a] *Materials Science and Engineering Department, IAAB, Universidad Carlos III de Madrid, 28911 Leganés, Spain*
[b] *Instituto de Ciencia de Materiales de Madrid, 28049 Madrid, Spain*

Received 14 November 2008; received in revised form 24 November 2008; accepted 20 January 2009
Available online 6 February 2009

Abstract

In this work the processing steps for producing YSZ thin tubes by means of powder extrusion moulding (PEM) technique are investigated. Different feedstocks were prepared from a commercial YSZ powder and a multicomponent thermoplastic binder system based in polypropylene and paraffin wax. The surface coating of YSZ powder with stearic acid in a high-performance dispersing instrument reduces the viscosity of the feedstock one order of magnitude respect to a feedstock with a same composition and un-coated powder. This fact allows increasing the solid loading up to 58 vol.% to obtain sintering tubes with densities higher than 97% and with wall thickness lower than 200 μm.

Keywords: A. Extrusion; C. Electrical conductivity; D. ZrO_2; E. Fuel cells; Tubular electrolyte

1. Introduction

Fuel cells convert chemical energy into electrical energy with high efficiency and low emission of pollutants [1,2]. Solid oxide electrolyte layer is one of the basic components in SOFCs operating at high temperature [3,4]. Yttria stabilized zirconia (YSZ) is widely used as the electrolyte in SOFCs due to its thermal stability, high ionic conductivity and good thermal expansion compatibility with the electrode materials [3,5]. The highest conductivity level of $(ZrO_2)_{1-x}(Y_2O_3)_x$ electrolyte is obtained when x is 0.08 [6,7].

Among various cell configurations studied and reported in the literature (tubular, planar, monolithic, radial in electrode and electrolyte supported configurations), tubular and planar cells have attracted the most attention in recent years. For a self-supported configuration, YSZ electrolyte requires a temperature of operation greater than 900 °C. However operation at this elevated temperature represents a major problem for planar SOFC configurations. On the contrary the tubular cell design developed by Westinghouse Electric Corporation offers the advantage of a seal-less generator design and cell-to-cell connection over the axial ceramic interconnection strip exposed to a fuel environment [4,8,9].

Several methods can be used to fabricate a tubular support [8,10]. Extrusion is a very economic process and effective technique to produce objects with constant cross-section such as rods and tubes [11,12]. Because extrusion is based on plastic forming, there exist certain mechanical requirements for extrusion to occur. The first requirement is flow. The material to be extruded must be plastic (or flowable) enough during the extrusion process to form the desired cross-section. The second requirement is green strength. After the material is extruded it must be strong enough to resist deformation either coming from its own weight (slumping) or from handling stresses. If these conditions are not met, good extrusion will not be obtained [13]. In this sense the binder technology will have a critical effect on PEM processes, since binders play a fundamental role in increasing fluidities and retaining shapes. According to the literature, the highest powder loading achieved is around 55 vol.% for YSZ mixtures with the binders based on wax systems and with PVA as a polymer component [14–16].

Although a few publications have appeared that describe the design and properties of fuel cells with tubular electrolyte, the extrusion method itself is only sporadically described in detail in the literature. For binders to be useful in thermoplastic extrusion, their rheology and the debinding behaviour must be

* Corresponding author. Tel.: +34 916249484; fax: +34 916249430.
E-mail address: alvar@ing.uc3m.es (A. Várez).

0272-8842/$34.00
doi:10.1016/j.ceramint.2009.01.008

known. The present contribution describes the optimization of the fabrication procedure for successfully extruding YSZ thin-wall tubes. It has been performed on the basis of previous experience on powder injection moulding (PIM) of ceramics such as alumina, ferrites and YSZ [17–19], and metals such as high speed steels [20,21]. Finally the conductivity properties of the sintered thin-wall tubes has been studied by impedance spectroscopy (IS) and compared with the conductivity of pellets of the same YSZ powder sintered at the same temperature.

2. Experimental procedure

2.1. Materials

A commercially available cubic YSZ ceramic powder, containing 8 mol% Y_2O_3 (Tosoh Corporation) was used as raw material. The average particle size of the powder is 0.6 μm and the reported surface area is 7 m^2/g. The binder used was a multicomponent mixture similar to that used in powder injection moulding. It is a thermoplastic binder and is constituted of three components which fulfil different functions: a backbone polymer that provides strength, a wax that provides high flowability to the binder, decreasing the viscosity at the processing temperature, and a surfactant to bridge between the binder and the powder (usually the surfactant also acts as a lubricant to help with tool release). In our case the organic binder consisted of polypropylene (PP), paraffin wax (PW) and stearic acid (SA). The PP used in this study has a melt flow index of 30 g/min (at 230 °C and 2.16 kg following ISO 1133:2005), this assures low viscosity of binder but good green strength of pieces. It was supplied by Repsol-YPF Company. PW and stearic acid were of commercial grade provided by Panreac. Some physical properties of the binder components are provided in Table 1. Densities were evaluated with a He Picnometer (Micromeritics Accupyc 1330) while thermal properties were determined with a Differential Scanning Calorimetry (DSC) using a PerkinElmer Dyamond instrument under a N_2 flow and a heating rate of 10 °C/min.

2.2. Mixing and compounding

As mentioned the prepared binders were based on polypropylene and paraffin wax in the optimal proportion of 50 PP–46 PW vol.%. The amount of stearic acid was selected to be 4 vol.% [19]. Binder components (PP, PW and SA) and YSZ powder were premixed in a Turbula mixer at room temperature. A second mixture was prepared in the same way but with a previous surface treatment of zirconia powders with the 4% of stearic acid, using a high-performance dispersing instrument (Miccra) at 20,000 min^{-1} for 15 min. After that, the dry powder was mixed in the Turbula mixer with the other components of the binder (PP and PW). Feedstock having different solid loading (55 and 58 vol.%) were prepared.

Table 1
Characteristics of the binder components.

Component	Density (g/cm^3)	T_m [a] (°C)	ΔH_m [b] (J/g)
Polypropylene	0.8858	163.8	100.5
Paraffin wax	0.8886	56.8	145.0
Stearic acid	1.0122	73.7	169.5

[a] Melting temperature.
[b] Melting enthalpy.

Afterwards, a twin screw extruder was used to prepare the feedstocks for the extrusion moulding of the samples. In order to obtain a feedstock with high homogeneity the mixture was extruded three times. The homogeneity was confirmed through density measurements of the extrudates. The temperature control was set to be 170–175–180 °C from barrel to nozzle at 40 r.p.m. The rheological characterization of all the mixtures prepared was performed in a Rheoflixer capillary rheometer (ThermoHaake) at 180 °C over a range of shear rates from 100 to 10,000 s^{-1} with temperature control of ±1 °C. The dimensions of the die were 30 mm length (L) and 1 mm diameter (D) (L/D ratio of 30).

2.3. Extrusion moulding

Continuous tube extrusion was performed on a single screw extruder (Rheomex) with temperatures from feed to nozzle between 170 and 180 °C. A home-designed extrusion die was connected to the extruder. The tubes were vertically extruded through a nozzle of 4 mm outer diameter and 3.5 mm inner diameter (i.e. a wall thickness of 0.5 mm).

2.4. Debinding and sintering

Removal of the binder was performed by a solvent debinding process followed by a thermal treatment. The solvent debinding was conducted in the optimal conditions of 60 °C and 3 h holding time. The details of the experimental procedures have been described in a previous paper [19]. Thermogravimetric analyses (TGA) were used to study the thermal debinding characteristics of the prepared binders. The TGA experiments were performed on a PerkinElmer TGA Pyrys1. Thermogravimetric experiments were performed from room temperature to 600 °C with a heating rate of 10 °C/min and air flow of 100 mL/min. The total amount of carbon in the debound parts was determined by elemental analysis performed with a LECO instrument.

The sintering process took place immediately after the debinding. The tubes were placed horizontally on an Al_2O_3 crucible and a vertically hung was not necessary to enable the tubes to remain straight during firing. Debound tubes were sintered at temperatures ranging from 1350 to 1650 °C with a soaking time of 2 h and a constant heating rate of 3 °C/min. For comparison uniaxially pressed disks (P = 200 MPa) of YSZ powder were sintered in the same conditions.

The sectional microstructures of extrusion moulding parts were observed using an optic microscope. The microstructure of the materials was evaluated in a Philips XL 30 scanning electron microscope operating at 15 kV, on polished and chemically etched surfaces. Sintered samples densities were measured by Archimedes method. Electrical measurements were carried out on Ag-electroded tubes. Ag slurries were

prepared diluting DUPONT Ag 5009 conductive paint in terpineol and then deposited on the YSZ substrates by the slurry coating process to produce the electrodes on both sides of the tubes. Impedance spectroscopy measurements were made under static air atmosphere using an Agilent E4980A LCR in the frequency range 20 Hz to 1 MHz. The applied electric field was kept below 1 V/cm to ensure linear electrical response. The temperature range used was 200–500 °C with 25 °C increment between subsequent steps. On the other hand the pellets sintered in the same conditions as the tubes, were polished in their larger faces and Pt electrodes were deposited by sputtering. The measuring conditions of the pellets were the same as for the tubes.

3. Results and discussion

3.1. Rheological behaviour

One of the aims when formulating feedstock for powder extrusion moulding is to maximize the solids loading in order to reduce the problems associated with binder elimination and the shrinkage during densification. In a first step, the volume fraction of powder in the moulding mixture was fixed at 55% which is the highest level of solid loading reported for YSZ feedstocks in powder injection moulding [14–16].

The rheological properties of feedstocks are crucial to evaluate the suitability for being extruded. The main problem in extruding thin-wall tubes is the tendency of the thin-wall profile to collapse. In this sense the rheological properties of the mixture being extruded must be such that no deformation of the plastic green body can occur due to own weight or to the necessary handling. When a thermoplastic mixture is used, the extruded green body solidifies immediately after the tube is cooled below the shaping nozzle. In contrast, a too high viscosity of the blend at the working temperature could obstruct the nozzle impeding the extrusion process. Fig. 1 gives the dependence of viscosity on shear rate for the feedstocks at the extrusion temperature (180 °C). The ceramic mixtures showed pseudoplastic behaviour and the viscosity decreased with the shear rate in the whole studied range. This behaviour is the most adequate for the injection or extrusion process. The viscosity at 100 s^{-1} was less than 1000 Pa s, the recommended value for PIM purpose [22].

As it can be seen in Fig. 1, for the mixtures with 55 vol.% of powder loading the flow behaviour of the feedstock prepared with stearic acid coated powders is basically identical to the feedstock with not coated YSZ powder, but the values are reduced almost one order of magnitude in all the shear rate range studied. This decrease in the viscosity is considerably higher than other reported for zirconia powder where the viscosity was slightly reduced at similar temperature [23] or the reduction was about 0.3 or 0.4 orders of magnitude with about 5 wt.% of SA [24]. This fact suggests that the decrease in the viscosity is not only determined by the SA coating and that the method of dispersion of the surfactant agent with the ceramic powders is decisive. In addition, this composition with powder coated, unlike of feedstock with not coated powder, did not present abrasion problems with the surface of the equipments. Fig. 2 shows the morphology of the untreated and treated YSZ powders. As it can be seen, large agglomerates were disintegrated by dispersion processes into primary particles and hard aggregates in the coated powders. This effect, together with the better dispersion promoted by the stearic acid, explains the decreasing of viscosity in feedstock prepared with SA recovery powder. As above mentioned, stearic acid is often used with ceramic particles as dispersive surfactant acting on the principle of stearic stabilization, but besides it also acts as a

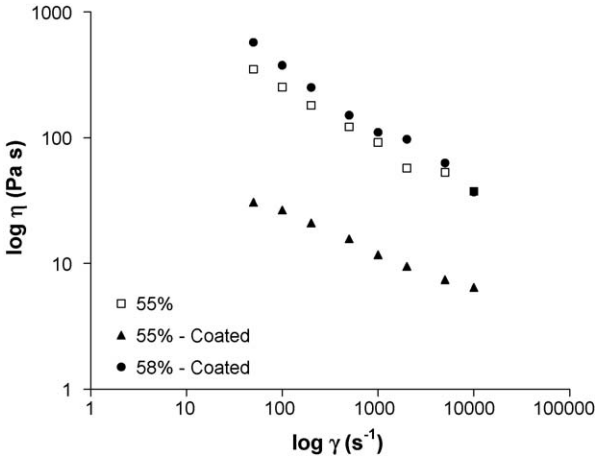

Fig. 1. Rheological behaviour at 180 °C for the different feedstocks prepared: with a powder loading of 55% and using coated and non-coated powders, and with a powder loading of 58% and SA-coated YSZ powder.

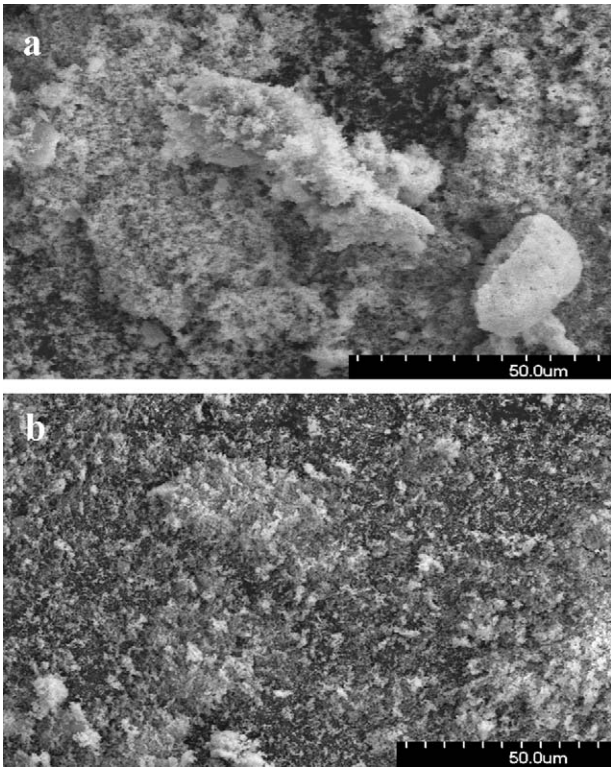

Fig. 2. Scanning electron micrographs of: (a) untreated and (b) treated YSZ powders.

wetting agent, reducing the viscosity of the ceramic mixture by breaking up the existing particle networks [23,25].

This decreasing in both the viscosity and the abrasion problems with the equipments when using SA-coated YSZ powder, allowed to increase the powder loading up to 58%, with the same binder composition (50 PP–46 PW vol.%, and YSZ coated with 4 SA vol.%). Fig. 1 shows the rheological behaviour of this new feedstock formulation and it is compared with the previous mixture formulated. The greater amount of ceramic powder for this mixture leads to an increase in the viscosity with respect to the other feedstock studied, however, the viscosity curve is still acceptable for PEM purpose and again it showed no abrasion problems with the surface of the equipments.

Taking into account these facts, the powder treated with SA and mixed with the binder 50 PP–46 PW vol.% (for a solid loading of 58 vol.%) was selected as the optimum feedstock in this study.

3.2. Debinding and sintering

Debinding is one of the most critical steps in PEM process since removing the organic binder from the moulded parts often gives rise to defects, especially when fine ceramic powder is used. Heating profiles have a strong influence on the formation of internal cracks in the moulded components.

According to this a combination of solvent and thermal debinding was carried out. First, an organic solvent (n-heptane) was used to extract soluble PW and SA in the tubes. After drying, a thermal debinding in air at atmospheric pressure was applied, in order to remove the polypropylene. The most suitable heating cycle was designed by means of thermogravimetrical analysis of the feedstock (see Fig. 3). The decomposition of the binder occurs gradually in a relative wide temperature range. Degradation starts at about 180 °C and finishes at about 500 °C, through two weight loss stages. The first weight loss stage, about 50 wt.% of the total loss in the temperature range of 180–350 °C is attributed to the degradation of paraffin wax and stearic acid in the binder system. The second stage between 350 and 500 °C is associated to the degradation of PP. The total weight loss percent (11 wt.%) corresponds to total organic component of the feedstock (10.9 wt.%). The heating cycle, used for binder removal, follows several steps: before 150 °C a relatively quick heating rate of 5 °C/min was chosen taking into account that higher heating rates will cause cracking in the samples and lower heating rates will unnecessarily increase the debinding time. Between 150 and 200 °C a slower heating rate, 2 °C/min, was used in order to degrade the residual low molecular weight components of the blend. Between 200 and 300 °C a slope of 5 °C/min was employed. A slower heating rate of 1 °C/min was determined as the optimum rate between 300 and 500 °C to prevent surface cracks and internal bubbles. Finally, the parts were kept at 500 °C for 1 h to completely burn out the organic components.

This combined solvent and thermal debinding process makes possible to obtain free defects tubes in a reduced time (11 h). This time is quite lower than that reported by other authors [13,26]. The complete elimination of the polymeric part was again confirmed through carbon elemental analysis of the brown parts. The carbon content of these parts was around 0.01%, indicative of a successful debinding process.

Fig. 4 depicts the evolution of the theoretical density of PEM and uniaxial pressed samples as a function of sintering temperature at a heating rate of 3 °C/min. Tubes free of defect could be obtained for all sintering temperatures. At approximately 1450 °C the plateau of the curve is achieved for both extruded tubes and compacted samples, obtaining densities higher than 97% of the theoretical. Nevertheless in pressed samples sintering seems to occur at slightly lower temperatures, probably because the density in the pressed green bodies is higher than in the tubes. The shrinkage of the tubes was approximately 40%, being the final wall thickness lower than 200 μm for all sintering temperatures. Fig. 5 shows a photograph of the tubes in the different steps: green body, debound and sintered at 1500 °C, and Fig. 6 shows the micrograph of the cross-section of a tube sintered at 1500 °C/2 h.

SEM micrographs of the tube and the compacted sample sintered at 1500 °C are shown in Fig. 7. The pressed sample

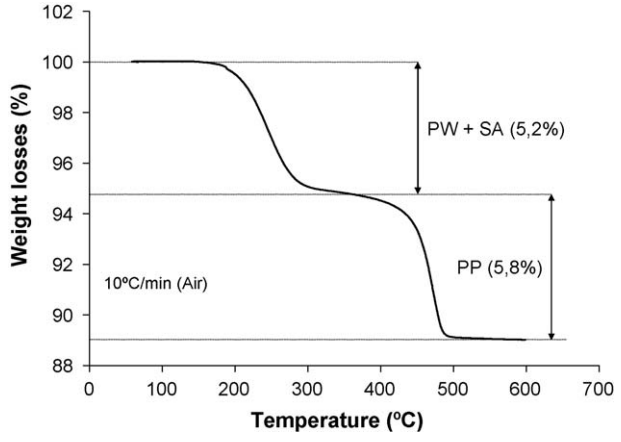

Fig. 3. Thermogravimetrical analysis (TGA) of the feedstock at a heating rate of 10 °C/min in air.

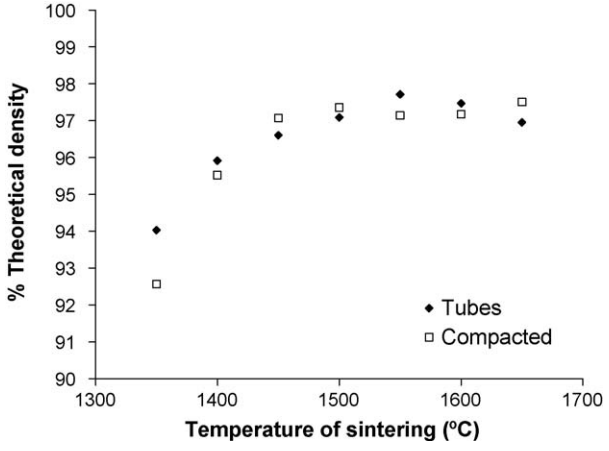

Fig. 4. Densification as a function of temperature for the compacted disks and the extruded tubes sintered for 2 h at temperatures from 1350 to 1650 °C.

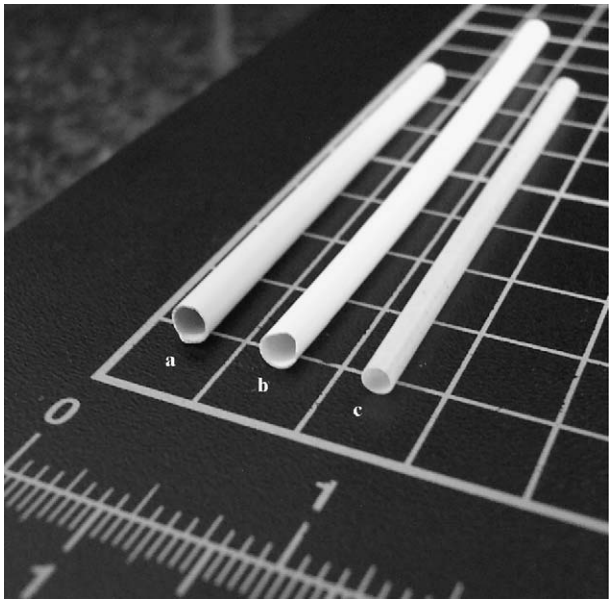

Fig. 5. Photograph of the tubes in the different steps: (a) green body, (b) debound and (c) sintered at 1500 °C.

contained tiny round pores mostly enclosed within the grains. The enclosed pores in grain centres are indicative of a rapid growth of grains during sintering. The average grain size was around 5 μm. In the micrograph of the sintered tube a more frequent occurrence of pores of up to 1 μm and smaller grains of an average size of 3 μm can be observed. There are also some big pores in the image, but these can be attributed to the pulling out of grains during the polishing treatment. The microstructure and density of the sintered tubes were largely dependent upon the preparation method of the green tubes. This microstructure could be improved by using the optimized extrudate procedures to obtain higher green densities in the tubes.

3.3. Characterization of properties.

Impedance spectroscopy measurements were performed at temperatures ranging from 200 to 500 °C. Fig. 8 shows the impedance plots at 300 °C, corresponding mainly to the bulk contribution, for both the extruded and the pressed samples. In the case of the pressed samples and for all the temperatures analyzed, the bulk and the grain boundary contributions could not be easily separated, which should be attributed to a highly homogeneous microstructure.

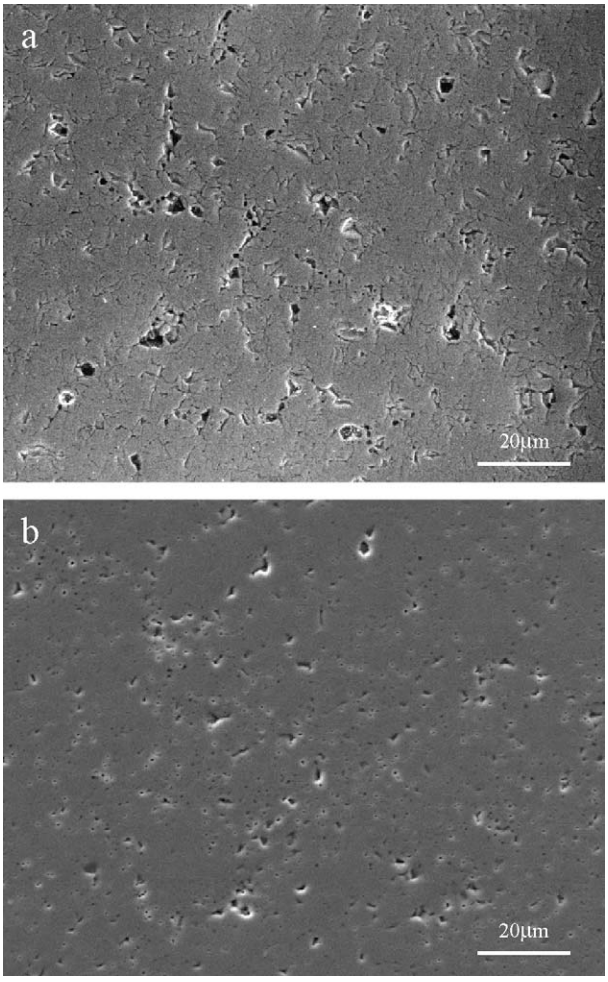

Fig. 7. SEM micrographs of polished and chemically etched surfaces of (a) extruded sample and (b) pressed sample sintered at 1500 °C.

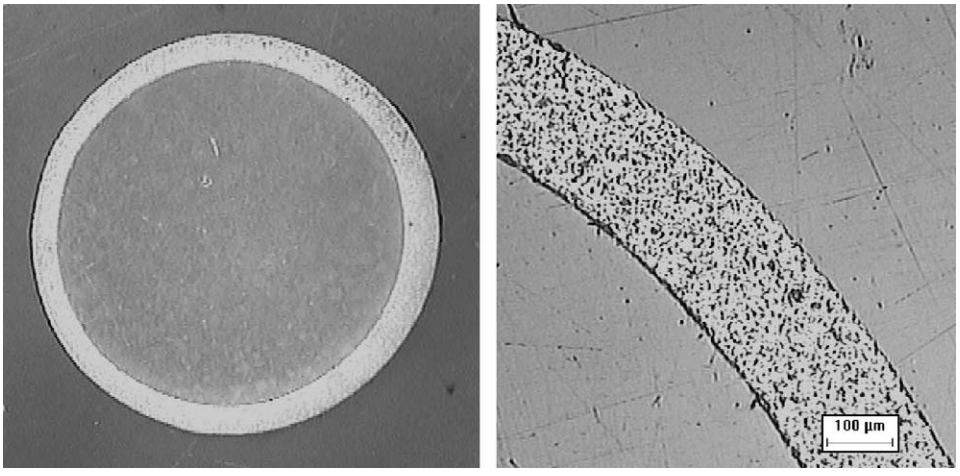

Fig. 6. Cross-section micrograph of a tube sintered at 1500 °C/2 h. Sample was polished and chemically etched to reveal the microstructure.

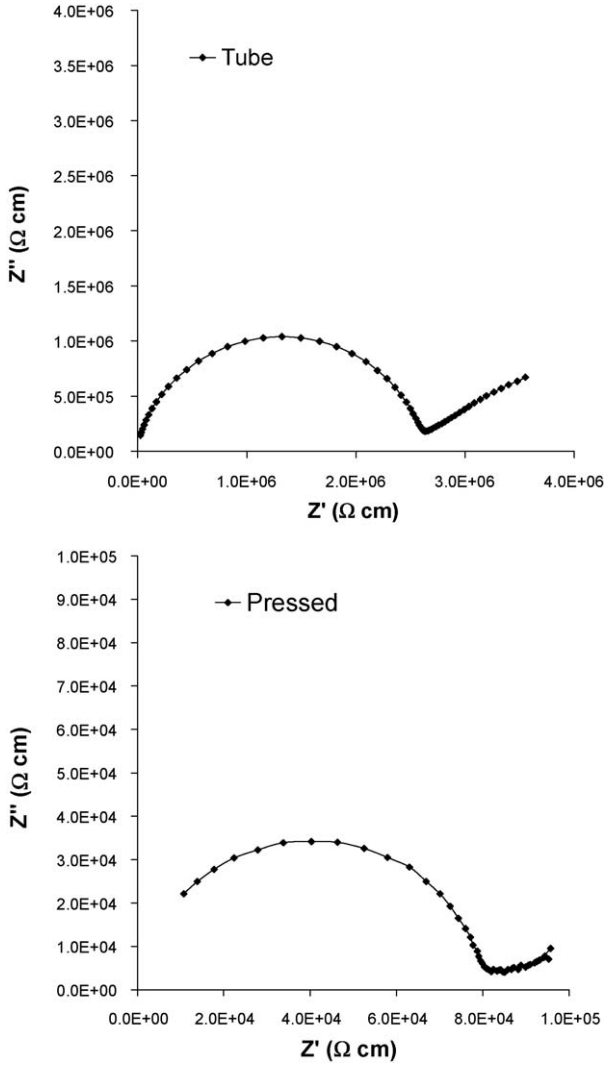

Fig. 8. Impedance spectra at 300 °C in air of the extruded and the pressed samples sintered at 1550 °C.

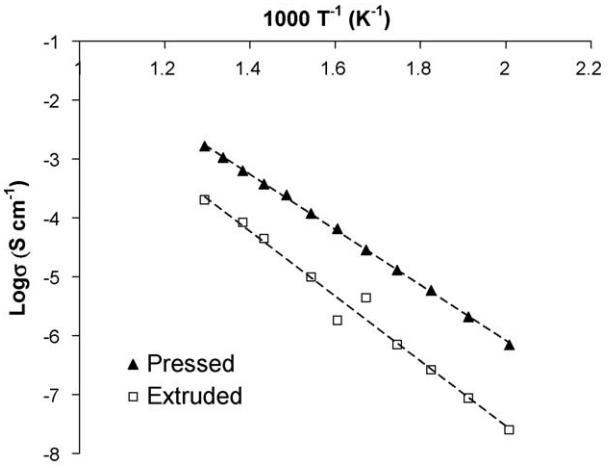

Fig. 9. Arrhenius plots of total conductivity for the extruded tubes and the pressed samples sintered at 1550 °C. The activation energy is 1.09 eV in the extruded tubes and 0.88 eV in the sintered pellets.

The total resistance was considered to be the sum of the grain boundary and the bulk resistances. Arrhenius plots of total conductivity for the compacted disks and the extruded tubes sintered at 1550 °C are depicted in Fig. 9. Conductivity of the tubes is one order of magnitude lower than the compacted disks. The activation energy for the d.c. conductivity is larger in the extruded tubes (1.09 eV) than in the sintered pellets (0.88 eV). Both values are in the range expected for oxygen vacancy conduction in YSZ. This difference in the ionic conductivity should be related to changes in the microstructure. The relative density of the tubes and the pellets is nearly the same (∼97%), but a larger amount of grain boundaries is present in the tubes due to its lower grain size (3 μm; 5 μm for the pellets). The presence of the intra-granular pores in the YSZ tubes prepared by extrusion, can also constraint the conductivity. These two effects can produce a decrease in the total conductivity, as well as an increase in the activation energy due to the larger influence of grain boundaries in the extruded tubes. Nevertheless the lowering of one order of magnitude seems too large for samples with 97% of density. At this stage it is possible to take into account other microstructural effects whose relative importance is increased when treating with thin ceramics. One of these effects is the difference between the real contact area and the macroscopic area. Kenjo and Nakagawa [27] demonstrated that the contact between a fired Au electrode and the ceramics is composed of multiple discrete spots (see Fig. 7 in Ref. [27]). The effect of the electrode coverage and microstructure (size of the contact spots and separation between them) is to increase the effective resistivity of the pellet as the thickness of the ceramic is reduced. The use of sputtered Pt electrodes on the polished surfaces of the YSZ pellets strongly increases the electrode coverage, preventing the contact spreading in discrete spots and producing an effective resistivity, closer to the true one of the bulk ceramic. Part of the increase in the resistivity observed in the extruded tubes can be related to an inappropriate microstructure of the Ag/YSZ tube contact, indicating that Ag slurry used to cover the tube surfaces should be optimized to avoid detrimental geometrical effects in the electric response [28].

4. Conclusions

A polymer-based system with high solid loading has been developed to obtain YSZ thin-wall tubes by thermoplastic powder extrusion moulding. The binder used to prepare the optimum feedstock was composed by polypropylene (50 vol.%), paraffin wax (46 vol.%) and stearic acid (4 vol.%). When the surface of the YSZ powder is previously treated with stearic acid in a high-performance dispersing instrument, the feedstock substantially reduces the viscosity (one order of magnitude), with respect to that of the non-treated powder. This allows an increase of the powder loading up to 58 vol.%. The debinding stage was optimized in order to decrease the total time of the process down to 11 h. A combination of solvent and thermal treatment led to achieve debound tubes free of defects. The achieved densities are similar to those of the pressed samples, with densities higher than 97% of the theoretical. Also a homogeneous microstructure is obtained, being the final wall thickness lower than 200 μm. The

conductivities values obtained in the extruded thin-wall tubes are slightly lower than in the pressed samples because of difference in the microstructure of both the ceramic and the electrode/electrolyte contact. The latter microstructural effect become more important as the thickness of the ceramic diminishes. Conductivity could be improved by using the optimized extrudate procedures to obtain higher green densities in the tubes and by improving the electrode/electrolyte contact.

Acknowledgements

The authors thank Spanish Agency CICYT (MAT2004-03070-C05-02 and MAT2007-64486-C07-06 projects) and Regional Government of Madrid (MATERYENER Programme, Project S-505/PPQ-0358) for financial support.

References

[1] B.C.H. Steele, A. Heinzel, Materials for fuel-cell technologies, Nature 414 (2001) 345–352.
[2] J.J.B. Goodenough, Y.H. Huang, Alternative anode materials for solid oxide fuel cells, J. Power Sources 173 (2007) 1–10.
[3] P. Singh, N.Q. Minh, Solid oxide fuel cells: technology status, Int. J. Appl. Ceram. Technol. 1 (2004) 5–15.
[4] P. Timakul, S. Jinawath, P. Aungkavattan, Fabrication of electrolyte materials for solid oxide fuel cells by tape-casting, Ceram. Int. 34 (2008) 867–871.
[5] P. Dahl, I. Kaus, Z. Zhao, M. Johnsson, M. Nygren, K. Wiik, T. Grande, M.A. Einarsrud, Densification and properties of zirconia prepared by three different sintering techniques, Ceram. Int. 33 (2007) 1603–1610.
[6] Y. Arachi, H. Sakai, O. Yamamoto, Y. Takeda, N. Imanishai, Electrical conductivity of the ZrO_2–Ln_2O_3 (Ln = lanthanides) system, Solid State Ionics 121 (1999) 133–139.
[7] S.P.S. Badwal, Zirconia-based solid electrolytes: microstructure, stability and ionic conductivity, Solid State Ionics 52 (1992) 23–32.
[8] N.M. Sammes, Y. Du, Fabrication and characterization of tubular solid oxide fuel cells, Int. J. Appl. Ceram. Technol. 4 (2007) 89–102.
[9] L. Blum, W.A. Meulenberg, H. Nabielek, R. Steinberger-Wilckens, Worldwide SOFC technology overview and benchmark, Int. J. Appl. Ceram. Technol. 2 (2005) 482–492.
[10] K. Kendall, N.Q. Minh, S.C. Singhal, Cell and stack designs, High temperature and solid oxide fuel cells, 2003, pp. 197–228.
[11] Y.H. Du, N.M. Sammes, Fabrication and properties of anode-supported tubular solid oxide fuel cells, J. Power Sources 136 (2004) 66–71.
[12] N.M. Sammes, Y. Du, R. Bove, Design and fabrication of a 100 W anode supported micro-tubular SOFC stack, J. Power Sources 145 (2005) 428–434.
[13] M. Trunec, Fabrication of zirconia- and ceria-based thin-wall tubes by thermoplastic extrusion, J. Eur. Ceram. Soc. 24 (2004) 645–651.
[14] W.J. Tseng, D. Chiang, Influence of molding variables on defect formation and mechanical strength of injection-molded ceramics, J. Mater. Process. Technol. 84 (1998) 229–235.
[15] D.M. Liu, W.J. Tseng, Binder removal from injection moulded zirconia ceramics, Ceram. Int. 25 (1999) 529–534.
[16] S. Lin, Near-net-shape forming of zirconia optical sleeves by ceramics injection molding, Ceram. Int. 27 (2001) 205–214.
[17] E. Rodríguez-Senín, A. Várez, B. Levenfeld, J.M. Torralba, M.A. París, Processing of Mn–Zn ferrites using mould casting with acrylic thermosetting binder, Powder Metall. 48 (2005) 249–253.
[18] P. Thomas-Vielma, A. Cervera, B. Levenfeld, A. Várez, Production of alumina parts by powder injection molding with a binder system based on high density polyethylene, J. Eur. Ceram. Soc. 28 (2008) 763–771.
[19] T. Jardiel, M.E. Sotomayor, B. Levenfeld, A. Várez, Optimisation of the processing of 8-YSZ powder by powder injection moulding for SOFC electrolytes, Int. J. Appl. Ceram. Technol. 5 (2008) 574–581.
[20] G. Herranz, B. Levenfeld, A. Várez, J.M. Torralba, Development of new feedstock formulation based on high density polyethylene for MIM of M2 high speed steels, Powder Metall. 48 (2005) 134–138.
[21] L.A. Dobrzanski, G. Matula, G. Herranz, A. Varez, B. Levenfeld, J.M. Torralba, Metal injection moulding of HS12-1-5-5 high-speed steel using a PW-HDPE based binder, J. Mater. Process. Technol. 175 (2006) 173–178.
[22] B.C. Mutsudy, D.H. Xhetty, Engineering Applications of Ceramics Materials, American Society for Metals Park, OH, 1985, pp. 89–116.
[23] F. Allaire, B.R. Marple, J. Boulanger, Injection-molding of submicrometer zirconia-blend formulation and rheology, Ceram. Int. 20 (1994) 319–325.
[24] W.J. Tseng, D.M. Liu, C.K. Hsu, Influence of stearic acid on suspension structure and green microstructure of injection-molded zirconia ceramics, Ceram. Int. 25 (1999) 191–195.
[25] M. Trunec, P. Dobsak, J. Cihlar, Effect of powder treatment on injection moulded zirconia ceramics, J. Eur. Ceram. Soc. 20 (2000) 859–866.
[26] J. Pusz, A. Smirnova, A. Mohammadi, N.M. Sammes, Fracture strength of micro-tubular solid oxide fuel cell anode in redox cycling experiments, J. Power Sources 163 (2007) 900–906.
[27] T. Kenjo, T. Nakagawa, Ohmic resistance of the electrode–electrolyte interface in Au/YSZ oxygen electrodes, J. Electrochem. Soc. 143 (1996) L92–94.
[28] R. Jiménez, F. Otálora, M. Kleitz, Efecto sobre la reacción de oxígeno de la forma y la microestructura del contacto electrodo-electrolito en electrodos a difusión interna en celdas de combustible de óxido sólido (SOFC), Bol. Soc. Esp. Cerám. Vidrio 38 (1999) 625–629.